Available online at www.sciencedirect.com
ScienceDirect
Journal of Photochemistry and Photobiology A: Chemistry 186 (2007) 135–142
Journal of Photochemistry and Photobiology A:Chemistry
www.elsevier.com/locate/jphotochem

Improved efficiency of a thiophene linked ruthenium polypyridine complex for dry dye-sensitized solar cells

Coralie Houarner-Rassin [a,b,1], Errol Blart [a], Pierrick Buvat [b,1], Fabrice Odobel [a,*]

[a] *Université de Nantes, Nantes Atlantique Universités, CNRS, Faculté des Sciences et des Techniques, Laboratoire de Synthèse Organique (LSO), UMR CNRS 6513, 2, rue de la Houssinière, BP 92208-44322 Nantes Cedex 3, France*
[b] *CEA/Le Ripault, Département Matériaux, BP16, 37260 Monts, France*

Received 8 June 2006; received in revised form 24 July 2006; accepted 29 July 2006
Available online 9 August 2006

Abstract

We report herein the preparation, the electrochemical, the absorption and the emission properties of a new heteroleptic bisterpyridine ruthenium complex. The first terpyridine is functionalized, on the 4′ position, by a phosphonic acid group and the second terpyridine bears in the 4′ position a *tert*-thiophenyl unit attached *via* an ethanyl spacer. The latter complex was tested in dye-sensitized solar cells using the liquid electrolyte (I_2/LiI/*tert*-butylpyridine/propylene carbonate) or the solid poly(3-octylthiophene) as a hole conductor. It displays an improved photovoltaic photoconversion efficiency compared to the analogous complex in which the *tert*-thiophene is directly linked to the terpyridine ligand. This study shows that the covalent attachment of a thiophene residue on the sensitizer is a promising strategy for the development of solid-state dye-sensitized solar cells and it highlights the benefit of introducing a non-conjugated spacer between the thiophenyl unit and the polypyridine ruthenium sensitizer.

Keywords: Dye-sensitized solar cell; Ruthenium sensitizer; Solid-state solar cell; Photoelectrochemistry; Thiophene

1. Introduction

Dye-sensitized solar cells (DSSCs) are very attractive photovoltaic devices because they represent a low-cost technology for the transformation of solar energy into electricity. This type of photovoltaic device has reached a 10–11% efficiency under AM 1.5 (100 mW/cm^2) irradiation but only when a liquid electrolyte is used (I_3^-/I^- in solution in a mixture of organic solvents) [1–3]. The presence of the liquid electrolyte inside the cell seriously limits the industrial development of this technology due to the poor long-term stability of the cells and the mass production complexity required for the hermetic sealing. Several strategies have been tested to replace the liquid electrolyte by solid polymer electrolytes [4,5], quasi-solid gel electrolytes [6] and inorganic [7,8] or organic [9–12] hole-transport materials. However, none of them have been able to reach the overall photovoltaic efficiency that is obtained with the liquid electrolyte. Although relative successes have been achieved, the fully satisfying solution to this issue is still to be found [13].

Low photovoltaic efficiencies of solid cells relying on a solid hole transporting material (HTM) are most certainly due, among other factors, to the poor diffusion of this material into the voids of the nanocrystalline titanium dioxide electrode [14]. Thus, the sensitizers located at the bottom of the TiO_2 pores are not active towards electricity production, because they are situated too far away from the HTM to electronically communicate with it. Besides this, the maximum photovoltage delivered by this type of cell corresponds to the potential difference between the conduction band energy of the semiconductor and the oxidation potential of the redox mediator. Therefore, another appealing feature of replacing the iodide/triiodide redox couple by another HTM stems from the observation that a large amount of energy is lost (about 0.5 eV) for the regeneration of the oxidized sensitizer ($S^+ + I^- \rightarrow S + I_3^-$). Using a HTM, such as polythiophene, with a more positive oxidation potential than iodide/triiodide redox couple can raise the photovoltage delivered by the cell and thereby the overall efficiency of the cell.

In this article, we report a new strategy consisting in wiring the sensitizer to the HTM. The covalent attachment of the HTM

* Corresponding author. Tel.: +33 2 51 12 54 29; fax: +33 2 51 12 54 02.
E-mail address: Fabrice.Odobel@univ-nantes.fr (F. Odobel).
[1] Tel.: +33 2 47 34 44 85.

1010-6030/$ – see front matter © 2006 Elsevier B.V. All rights reserved.
doi:10.1016/j.jphotochem.2006.07.022

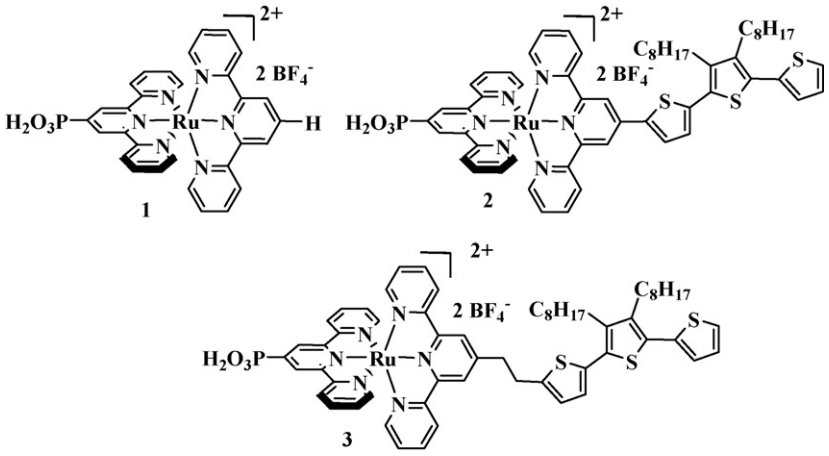

Scheme 1. Structure of the ruthenium complexes at the focus of the present study.

to the dye should ensure that all the sensitizers will be able to exchange holes with the counter-electrode through the HTM (Scheme 1). The hole transporting material which is the focus of the present study is oligothiophene. The group of Yanagida has shown that the "in situ" electrochemically polymerized pyrrole of bis-EDOT (EDOT: 3,4-ethylenedioxythiophene) can indeed be used to prepared solid-state DSSCs with interesting performance [15].

In a previous article, we showed that the direct attachment of a bis or *tert*-thiophene chain to a polypyridine ruthenium sensitizer, such as **2**, leads to an unexpectedly low photovoltaic system most probably due to the low electron injection efficiency [16]. We rationalized this previous finding by the fact that the extended π-conjugation between terpyridine and the thiophenyl unit stabilizes it LUMO orbital. As a result, the MLCT excited state involves this latter ligand and not the ligand that bears the anchoring group and that is bound to TiO_2 surface. Finally, the electronic coupling between the sensitizer and the TiO_2 is certainly decreased and induces thus a lower electron injection quantum yield.

In the present work, we propose supplementary interpretations for the low quantum yield of electron injection for the sensitizer **2** and we report the preparation and the study of the new system **3** in which the photovoltaic performances are improved as compared to unsubstituted complex **1**.

2. Experimental

2.1. General methods

^1H and ^{13}C NMR spectra were recorded on a Bruker ARX 300 MHz spectrometer. Chemical shifts for ^1H NMR spectra are referenced relative to residual protium in the deuterated solvent ($CDCl_3$ $\delta = 7.26$ ppm, MeOD $\delta = 3.31$ ppm, CD_3CN $\delta = 1.94$ ppm). Mass spectra were recorded on a EI-MS HP 5989A spectrometer or on a JMS-700 (JEOL LTD, Akishima, Tokyo, Japan) double focusing mass spectrometer of reversed geometry equipped with electrospray ionization (ESI) source.

Thin-layer chromatography (TLC) was performed on aluminum sheets precoated with Merck 5735 Kieselgel $60F_{254}$. Column chromatography was carried out either with Merck 5735 Kieselgel 60F (0.040–0.063 mm mesh). Air sensitive reactions were carried out under argon in dry solvents and glassware. Chemicals were purchased from Aldrich and used as received. Compounds [1,1′-bis(diphenylphosphino)ferrocene]dichloropalladium [17], tris(dibenzylideneacetone)dipalladium [18], 5-bromo-3′,4′-dioctyl-2,2′:5′,2″-*tert*-thiophene [16], 4′-bromo-2,2′:6′,2″-terpyridine [19] and 4′-diethylphosphonate-2,2′:6′,2″-terpyridine ruthenium (III) trichloride [20] were prepared according to literature methods.

UV–vis absorption spectra were recorded on a UV-2401PC Shimadzu spectrophotometer. The electrochemical measurements were performed with a potentiostat-galvanostat MacLab model ML160 controlled by resident software (Echem v1.5.2 for Windows) using a conventional single-compartment three-electrode cell. The working electrode was a Pt wire of 10 mm, the auxiliary was a Pt wire and the reference electrode was the saturated potassium chloride calomel electrode (SCE). The supported electrolyte was 0.1N Bu_4NPF_6 in DMF and the solutions were purged with argon before the measurements. All potentials are quoted relative to SCE. In all the experiments the scan rate was 100 mV/s for cyclic voltammetry and 15 Hz for pulse voltammetry.

Fluorescence spectra were recorded on a SPEX Fluoromax fluorimeter and were corrected for the wavelength dependent response of the detector system.

2.2. Preparation of the compounds

2.2.1. 5-(Trimethylsilylethynyl)-3′,4′-dioctyl-2,2′:5′,2″-tert-thiophene (*5*)

A Schlenk tube was charged with 150 mg (0.27 mmol) of 5-bromo-3′,4′-dioctyl-2,2′:5′,2″-*tert*-thiophene, 57 mg (0.21 mmol) of triphenylphosphine and 82 mg (0.82 mmol) of *i*-propylamine in 20 mL of dry triethylamine. The mixture was degassed by pumping and flushing with argon on the vacuum line and then 28 mg (0.03 mmol) of tris(dibenzylideneacetone)dipalladium, 23 mg (0.12 mmol) of copper iodide(I) and 80 mg (0.82 mmol) of trimethylsilylacethylene were added. The mixture was heated to 70 °C for 16 h. After

cooling to room temperature, the solvent was evaporated under vacuum. Purification was performed by column chromatography on silica gel with petroleum ether to yield **5** as a yellow solid (120 mg, 76%).

^{1}H NMR ($CDCl_3$, 300 MHz): $\delta = 7.32$ (dd, $^3J = 6.3$ Hz, $^4J = 1$ Hz, 1H), 7.18 (d, $^3J = 3.8$ Hz, 1H), 7.14 (dd, $^3J = 3.6$ Hz, $^4J = 1$ Hz, 1H), 7.07 (dd, $^3J = 3.6$ Hz, $^3J = 6.3$ Hz, 1H), 6.98 (d, $^3J = 3.8$ Hz, 1H), 2.70 (m, 4H), 1.25–1.60 (m, 24H), 0.90 (m, 6H), 0,10 (s, 9H). ^{13}C NMR ($CDCl_3$, 300 MHz): $\delta = 140.6$; 140.2; 137.9; 135.9; 133.0; 130.4; 129.2; 127.3; 126.1; 125.5; 125.2; 122.5; 97.5; 99.9; 31.9; 30.8; 30.6; 29.9; 29.2; 29.0; 28.2; 28.1; 27.7; 22.7; 14.1; 0. MS (EI): *m/z* (%) = 568 (100, $M^{+\bullet}$), 371 (24).

*2.2.2. 5-(Ethynyl)-3′,4′-dioctyl-2,2′:5′,2″-tert-thiophene (**6**)*

A solution of potassium carbonate (280 mg, 0.99 mmol) in methanol (6 mL) was added to 120 mg of 5-(Trimethylsilylethynyl)-3′,4′-dioctyl-2,2′:5′,2″-*tert*-thiophene **5** (0.2 mmol) in CH_2Cl_2 (3 mL). The solution was allowed to stir at room temperature for 5 h before being poured into water. The aqueous solution was extracted with dichloromethane and the organic layer was dried over magnesium sulphate, filtered and concentrated under vacuum. No further purification was necessary to yield **6** as yellow solid (100 mg, 99%).

^{1}H NMR ($CDCl_3$, 300 MHz): $\delta = 7.32$ (dd, $^3J = 5.1$ Hz, $^4J = 0.9$ Hz, 1H), 7.22 (d, $^3J = 3.9$ Hz, 1H), 7.14 (dd, $^3J = 3.6$ Hz, $^4J = 0.9$ Hz, 1H), 7.06 (dd, $^3J = 3.6$ Hz, $^3J = 5.1$ Hz, 1H), 6.98 (d, $^3J = 3.9$ Hz, 1H), 3.41 (s, 1H), 2.68 (m, 4H), 1.25–1.60 (m, 24H), 0.90 (m, 6H). ^{13}C NMR ($CDCl_3$, 300 MHz): $\delta = 140.8$; 140.3; 138.2; 135.9; 133.4; 131.3; 130.5; 128.8; 127.4; 126.1; 125.5; 125.2; 122.1; 82.2; 31.9; 30.7; 29.9; 29.2; 29.0; 28.2; 28.1; 27.7; 22.7; 14.1. MS (EI) : *m/z* (%) = 496 (100, $M^{+\bullet}$), 299 (50).

*2.2.3. 4′-Diethylphosphonate-2,2′:6′,2″-terpyridine-(4′-bromo-2,2′:6′,2″-terpyridine) ruthenium(II) di-tetrafluoroborate (**9**)*

A suspension of 4′-diethylphosphonate-2,2′:6′,2″-terpyridine ruthenium(III) trichloride (208 mg, 0.36 mmol) and $AgBF_4$ (185 mg, 1 mmol) was heated to 60 °C for 2 h in acetone (25 mL). After cooling to room temperature, the solution was filtered to remove AgCl and the filtrate was placed in a round bottom flask with *n*-butanol (25 mL). Acetone was evaporated under vacuum and the solution was degassed. A 90 mg (0.46 mmol) of 4′-bromo-2,2′:6′,2″-terpyridine was added and the resulting mixture was refluxed for 6 h. After cooling to room temperature, the solvent was evaporated under vacuum. The crude product was purified by column chromatography on silica gel, eluted with pure acetone and then with increasing gradients of water and saturated KNO_3 solution in acetone (starting from acetone/H_2O/KNO_3 90:10:0, until 79:20:1), to give a red product. The solid was dissolved in methanol and treated with $NaBF_4$ solution to precipitate **9** as a red solid (236 mg, 80%).

^{1}H NMR (CD_3CN, 300 MHz): $\delta = 8.93$ (s, 2H), 8.96 (d, $^3J = 13.5$ Hz, 2H), 8.57 (d, $^3J = 7.5$ Hz, 2H), 8.42 (d, $^3J = 7.5$ Hz, 2H), 7.86 (m, 4H), 7.35 (m, 2H), 7.27 (m, 2H), 7.11 (m, 4H), 4.33 (m, 4H), 1.42 (t, 6H). ^{13}C NMR (CD_3CN/MeOD (90:10), 300 MHz): $\delta = 158.19$; 157.58; 156.56; 153.69; 153.33; 139.40; 139.27; 136.64; 132.54; 128.94; 127.94; 126.03; 64.77; 16.97. HRMS-ESI (*m/z*): calcd for $C_{34}H_{30}B_2F_8N_6O_3PRuBr = 391.0172$ found = 391.0170.

*2.2.4. 4′-Diethylphosphonate-2,2′:6′,2″-terpyridine-(4′-[5-(ethynyl)-3′,4′-dioctyl-2,2′:5′,2″-tert-thiophene]-2,2′:6′,2″-terpyridine) ruthenium(II) di-tetrafluoroborate (**10**)*

A Schlenk tube was charged with 98 mg (0.2 mmol) of compound **6**, 96 mg (0.1 mmol) of complex **9** and 1 mL of dry triethylamine in 6.5 mL of dry DMF. The mixture was degassed by pumping and flushing with argon on the vacuum line and then 15 mg (0.02 mol) of [1,1′-bis(diphenylphosphino) ferrocene]dichloro-palladium and 4 mg (0.02 mmol) of copper iodide(I) was added. The mixture was heated to 90 °C for 16 h. After cooling to room temperature, the desired complex was precipitated by addition of $NaBF_4$ solution. The suspension was filtered and dried under vacuum. The crude product was purified by column chromatography on silica gel, eluted with pure acetonitrile and then with increasing gradients of water and saturated KNO_3 solution in acetonitrile (starting from acetonitrile/H_2O/KNO_3 100:0:0, until 79:20:1), to give a red product. The solid was dissolved in methanol and treated with $NaBF_4$ solution to precipitate **10** as a red solid (50 mg, 40%).

^{1}H NMR (CD_3CN, 300 MHz): $\delta = 9.0$ (d, $^3J = 13.5$ Hz, 2H), 8.93 (s, 2H), 8.72 (d, $^3J = 7.8$ Hz, 2H), 8.57 (d, $^3J = 7.8$ Hz, 2H), 7.97 (m, 4H), 7.65 (d, $^3J = 3.9$ Hz, 1H), 7.49 (m, 2H), 7.38 (m, 2H), 7.30–7.15 (m, 8H), 4.42 (m, 4H), 2.77 (t, 4H), 2.68 (t, 4H), 1.25-1.67 (m, 26H), 0.88 (m, 6H). ^{13}C NMR (CD_3CN, 300 MHz): $\delta = 158.3$; 156.6; 156.5; 155.9; 153.8; 153.4; 142.7; 141.6; 141.4; 139.4; 139.3; 132.1; 132.2; 129.4; 128.9; 128.7; 127.4; 126.1; 126.0; 125.7; 92.5; 91.4; 32.6; 31.3; 30.4; 29.9; 29.0; 23.4; 16.9; 16.8; 14.4. HRMS-ESI (*m/z*): calcd for $C_{64}H_{69}B_2F_8N_6O_3PRuS_3 = 599.1687$ found = 599.1690.

*2.2.5. 4′-Diethylphosphonate-2,2′:6′,2″-terpyridine-(4′-[5-(ethyl)-3′,4′-dioctyl-2,2′:5′,2″-tert-thiophene]-2,2′:6′,2″-terpyridine) ruthenium(II) di-tetrafluoroborate (**11**)*

A three neck round bottom flask was charged with 80 mg (0.06 mmol) of complex **10** in 12 mL of dry methanol. The mixture was degassed by pumping and flushing with argon on the vacuum line and then 40 mg (0.06 mmol) of Pd/C (20%, w/w) was added before the introduction of H_2. The mixture was vigorously stirred under hydrogen atmosphere for 16 h at room temperature. The reaction mixture was filtered on celite. After removal of the solvent, the crude product was purified by size exclusion column chromatography on Sephadex LH-20 as stationary phase to yield **11** as an orange solid (56 mg, 70%).

^{1}H NMR (CD_3CN + 1 drop of MeOD, 300 MHz): $\delta = 8.93$ (d, $^3J = 13.5$ Hz, 2H), 8.62 (d, $^3J = 7.8$ Hz, 2H), 8.57 (s, 2H), 8.40 (d, $^3J = 7.8$ Hz, 4H), 7.88 (m, 4H), 7.41 (d, $^3J = 3.9$ Hz, 1H), 7.31(m, 2H), 7.27 (m, 2H), 7.13–7.00 (m, 8H), 4.42 (m, 4H), 3.5 (m, 4H), 2.77 (t, 4H), 2.68 (t, 4H), 1.25–1.67 (m, 26H), 0.88 (m, 6H). ^{13}C NMR (CD_3CN + 1 drop of MeOD, 300 MHz): $\delta = 158.6$; 158.3; 156.5; 155.0; 153.6; 152.8; 144.2; 141.0; 139.1; 138.8; 128.5; 128.1; 127.4; 127.0; 126.7; 125.8; 125.1; 64.4; 38.2; 32.3; 31.1; 30.1; 29.7; 28.4; 23.1; 16.9; 16.8; 14.2. HRMS-ESI (*m/z*): calcd for $C_{64}H_{73}B_2F_8N_6O_3PRuS_3 = 606.1843$ found = 606.1853.

*2.2.6. 4′-Phosphonic acid-2,2′:6′,2″-terpyridine-(4′-[5-(ethyl)-3′,4′-dioctyl-2,2′:5′,2″-tert-thiophene]-2,2′:6′,2″-terpyridine) ruthenium(II) di-tetrafluoroborate (**3**)*

To a solution of the previous complex **11** (50 mg, 0.36 mmol) in freshly distilled DMF (5 mL) was carefully added an excess of dry trimethylsilyl bromide (290 mg, 2 mmol) under argon. The mixture was heated at 50 °C for 36 h under argon. After cooling to room temperature, the desired complex was precipitated by addition of dichloromethane. The suspension was filtered, washed with dichloromethane and dried under vacuum. The solid was dissolved in methanol and treated with $NaBF_4$ solution to precipitate **3** as an orange solid (40 mg, 90%).

^{1}H NMR (MeOD, 300 MHz): $\delta = 9.16$ (d, 2H, $^3J = 13.5$ Hz,), 8.67 (d, 2H, $^3J = 7.8$ Hz), 8.57 (s, 2H), 8.40 (d, 4H, $^3J = 7.8$ Hz), 7.83 (m, 4H), 7.39 (d, $^3J = 3.9$ Hz, 1H), 7.33 (m, 2H), 7.27 (m, 2H), 7.13–7.00 (m, 8H), 3.5 (m, 4H), 2.77 (t, 4H), 2.68 (t, 4H), 1.25–1.67 (m, 20H), 0.88 (m, 6H).

2.3. Preparation and characterization of the photoanodes

Conductive glass substrates (F-doped SnO_2 purchased from Solaronix Co.) were cleaned with water, rinsed with acetone and ethanol and dried in a nitrogen stream. Then, transparent nanocrystalline TiO_2 films were prepared by doctor blading the paste purchased from Solaronix Co. (colloidal anatase, particle size of approx. 13 nm), followed by sintering at 450 °C for 30 min in air. After cooling to room temperature, the films were immersed in a 3×10^{-4} M dye solution for 16 h in room temperature. Subsequently, the hole transport layer (40 g L^{-1} poly-(3-octylthiophene) in toluene) was applied by spin-coating and 200 nm thick gold electrodes were vacuum evaporated on the top by PVD. The current–voltage characteristics of the resulting photovoltaic cell were measured by a Keithley model 2400 digital source meter with an halogen lamp calibrated to AM1.5 (air mass) intensity (1000 W m^{-2}).

3. Results and discussion

3.1. Design and preparation of the system **3**

As shown by Barigelletti and coworkers [21–24] and others [25–27], the direct attachment of a thiophenyl moiety to a polypyridyl ruthenium complex induces a stabilization of the LUMO orbital of the functionalized polypyridine ligand and thus a red-shift of the MLCT transition. Since this phenomenon is certainly at the origin of a low injection quantum yield of the sensitizer, we investigated the effect of interrupting the π-conjugation between the ruthenium complexes and the thiophenyl unit. This led us to prepare the system **3** in which the thiophene is linked to the terpyridine complex by ethanyl group. From synthetic point of view, the compound **3** could be prepared

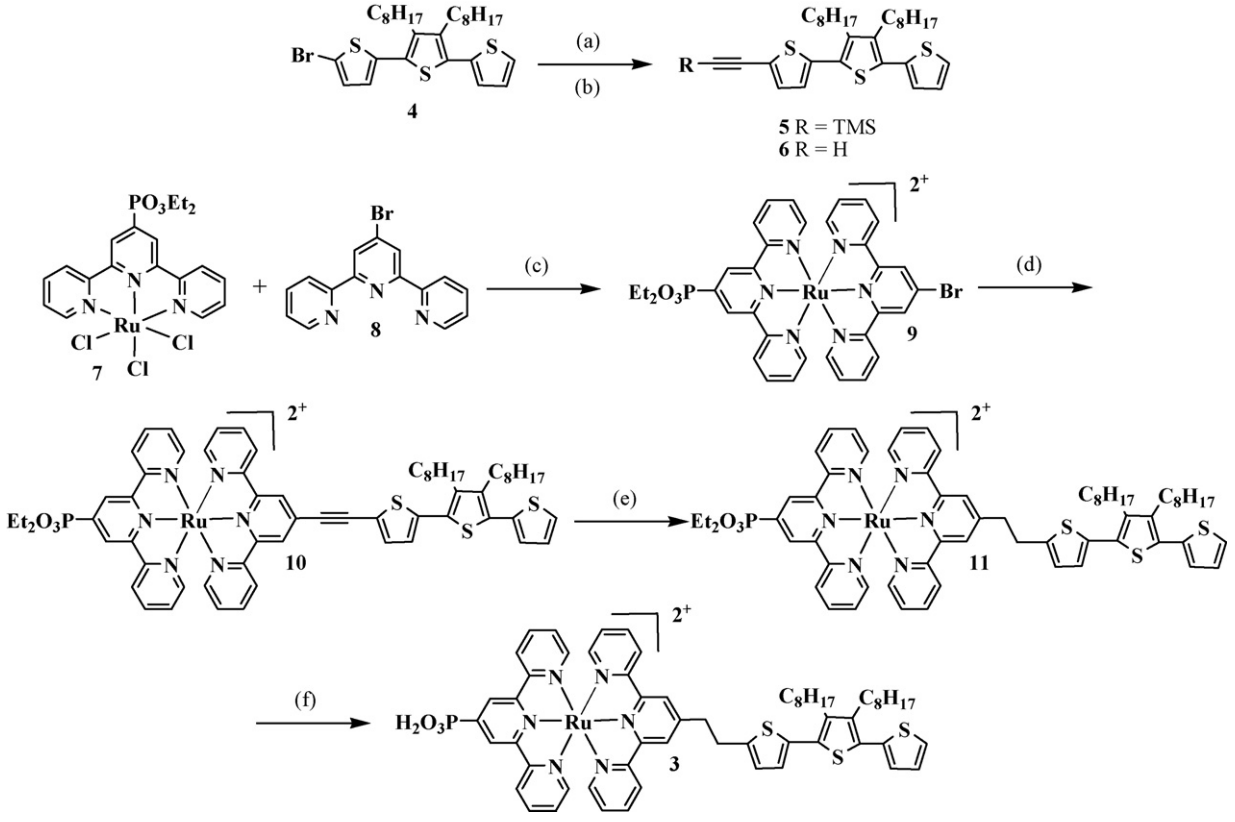

Scheme 2. Synthetic route for the preparation of complex **3**. Reagents and conditions: (a) trimetylsilylacethylene, PPh_3, *i*-Pr_2NH, CuI, $Pd_2(dba)_3$-$CHCl_3$, Et_3N, 70 °C, 16 h (76%); (b) K_2CO_3, MeOH/CH_2Cl_2, RT, 5 h (99%); (c) (i) **7**, $AgBF_4$, acetone, reflux, 2 h and (ii) **8**, *n*-BuOH, reflux, 6 h (80%); (d) **6**, CuI, Et_3N, $Pd(dppf)Cl_2$, DMF, 90 °C, 16 h (40%); (e) H_2, Pd/C, MeOH, RT, 16 h (70%); (f) (i) Me_3SiBr, DMF, 50 °C, 36 h and (ii) MeOH, RT (90%). The counteranions of the charged molecules are BF_4^-.

Table 1
Photophysical and electrochemical properties of complexes **1**–**3**

Complex	Absorption[a]	Emission		Electrochemistry[b]			
	λ_{max} (nm) (M^{-1} cm^{-1})	λ_{max} (nm)[c]	E_{00} (^{3}MLCT) (eV)[d]	$E_{1/2}$ (Ru^{III}/Ru^{II})[e]	E_{ap} ($T^{\bullet+}/T$)[f]	$E_{1/2}$ ($trp/trp^{\bullet-}$)[e]	$E^*_{1/2}$ (Ru^{III}/Ru^{II})[g]
1	274 (43000), 312 (57000), 482 (16400)	616	2.01	1.32		−1.22	−0.69
2	274 (39900), 309 (42600), 373 (16100), 505 (30700)	716	1.73	1.32	1.21	−1.15	−0.52
3	273 (62500), 308 (73300), 481 (20700)	607	2.04	1.35	1.21	−1.22	−0.69

[a] Recorded in acetonitrile at room temperature.
[b] Potentials determined by cyclic voltammetry in 0.1 M tetrabutylammonium hexafluorophosphate in acetonitrile solution with the scan rate 100 mV/s, all potential are referred vs. saturated calomel electrode (SCE).
[c] Recorded in rigid ethanol matrix at 77 K.
[d] E_{00} calculated from the maximum intensity emission wavelength according to the equation: E (eV) = 1240/λ_{em} (nm).
[e] $E_{1/2} = E_{ap} - E_{cp}$ with E_{ap} is the anodic peak potential and E_{cp} is the cathodic peak potential.
[f] E_{ap} is the anodic peak potential corresponding to an irreversible process. T = thiophenyl unit.
[g] Excited-state redox potential determined according to $E^*_{1/2}$ (Ru^{III}/Ru^{II}) = $E_{1/2}$ (Ru^{III}/Ru^{II}) − $^3E_{00}$ (MLCT).

by hydrogenation of a triple bond that can be introduced from Sonogashira cross-coupling reaction (Scheme 2).

Briefly, the synthesis of **3** starts with the preparation of complex **9** by reacting the known ethylphosphonate terpyridine trichloro ruthenium complex **7** [20] with bromoterpyridine **8** [19]. A Sonogashira cross-coupling reaction is then performed directly on complex **9** using Tor's reaction conditions [28]. Finally, the triple bond was reduced by hydrogen in the presence of palladium on charcoal and the ethylphosphonate group was transesterified by trimethylbromosilane and hydrolyzed in methanol to afford complex **3**.

3.2. Absorption and emission spectroscopy

The UV–vis absorption and emission characteristics of the complexes **1**–**3** are gathered in Table 1. The absorption spectra of the complexes are shown in Fig. 1.

The spectra of complexes **1**–**3** exhibit the usual broad MLCT absorption band around 500 nm, the ligand-centered π–π* transitions between 250 and 350 nm and in the near UV region, a π–π* transition located on the *tert*-thiophene. The MLCT transition is red-shifted in complex **2** compared to complexes **1** and **3** indicating effective π-conjugation between the terpyridine and *tert*-thiophene in **2**. In complex **3**, this π–π* transition of *tert*-thiophene is around 350 nm and is partly covered by the π–π* transition of the pyridine units. Interestingly, the MLCT transition in complex **3** is located at a similar position as that of reference complex **1**, which confirms that the triple bond has been reduced and that π-conjugation between the terpyridine and the *tert*-thiophene has been interrupted (Table 1).

The luminescence spectra of the complexes were also recorded to estimate the energy level of the triplet MLCT state. The data are collected in Table 1. In agreement with the blue-shift of the absorption MLCT transition in complex **3** relative to that in complex **2**, the emission spectrum of **3** indicates that the MLCT excited-state lies at a higher energy level than that of **2**, which is rather similar to that found in the reference complex **1**. The luminescence spectra of complexes **1** and **2** were recorded at room temperature in three different solvents of increasing polarity (THF, $\varepsilon_s = 7.6$; CH_3CN, $\varepsilon_s = 38.8$; DMSO, $\varepsilon_s = 47.2$) where ε_s refers to the solvent dielectric constant (Table 2). The emission spectrum of complex **1** is red-shifted when the polarity of the solvent is increased. This result is in agreement with a charge transfer excited-state such as an MLCT state which is stabilized by electrostatic interaction of the solvent dipoles with the strongly polar excited-state. Surprisingly, for complex **2** the emission wavelength is almost independent of the polarity of the medium which tends to indicate that the charge distribution in the excited-state has weakly changed as compared to the ground state.

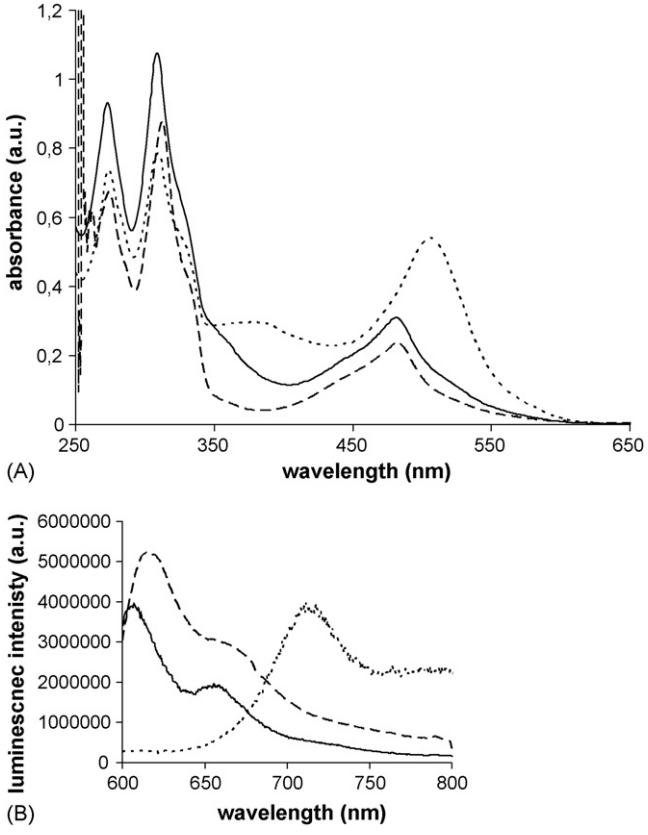

Fig. 1. Absorption spectra recorded at room temperature in acetonitrile (A) and phosphorescence spectra recorded in rigid ethanol matrix at 77 K (B). Complex **1** (- - -), complex **2** (· · ·), and complex **3** (—).

Table 2
Maximum emission wavelength of the phosphorescence spectra of the complexes **1** and **2** recorded in degassed solvent with 0.01 M of *n*-Bu_4NOH at room temperature

Complex	λ_{em} (nm)		
	THF	CH_3CN	DMSO
1	630	638	655
2	769	768	768

With reference to previous work of Barigelletti and coworkers [23] on ruthenium bipyridine complexes substituted with oligothiophene-ethynylene units, these results suggest that the emitting state in complex **2** is most probably not a pure triplet MLCT excited state as in **1** but a triplet $^3\pi$–π^* state localized on the terpyridine-thiophene unit. The conjugation between the terpyridine and the thiophene has probably two effects. First, it decreases the HOMO-LUMO energy gap on the ligand and consequently the energy level of the $^1\pi$–π^* and of the $^3\pi$–π^* state of the *tert*-thiophene unit. Second, the presence of the nearby ruthenium cation increases the spin–orbit coupling which promotes the intersystem crossing from a singlet to a triplet state. As a result, the lowest excited-state in complex **2** is not the triplet MLCT state but a triplet $^3\pi$–π^* state most certainly localized on the thiophene-terpyridine ligand. This property could explain the much weaker photovoltaic performances of complex **2** in DSSC, because electron injection from $^3\pi$–π^* is most likely less efficient than from the MLCT. First, because the thiophene based $^3\pi$–π^* transition is not a strong charge transfer as is the MLCT and second the thiophene terpyridine unit is further away from the acceptor state (conduction band of titanium dioxide). In the new complex **3**, the interrupted π-conjugation has restored the expected energetics of the excited states of the sensitizer.

3.3. Electrochemistry

The redox potentials of the complexes were measured by cyclic voltammetry and the data are gathered in Table 1. Three important pieces of information can be drawn from these measurements. First, in complex **3** the first reduction process, which corresponds to electron injection into the most reduceable terpyridine ligand, occurs at the same potential as that measured in complex **1** (−1.22 V versus SCE). It can be concluded that this process affects the phosphonic acid terpyridine ligand and indicates that the LUMO orbital of the complex is therefore located on this fragment. Second, in complex **3** the first oxidation is an irreversible process involving the *tert*-thiophene centre. This ordering of oxidation potentials implies that the oxidized ruthenium(III) complex upon electron injection in the empty Ti(3d) states manifold of the TiO_2 conduction band, could in principle be reduced by the nearby *tert*-thiophene unit (Ru^{III}-*tert*-thioph → Ru^{II}-*tert*-thioph$^+$). Third, the calculation of the excited-state oxidation potentials ($E^*_{1/2}$ (Ru^{III}/Ru^{II})) of the sensitizers indicate that complex **2** exhibits significant lower reducing ability than the complexes **1** or **3** ($\Delta E = 170$ mV). Although the potential of the conduction band potential of TiO_2 shifts with the pH and is affected by the chemisorbed species on its surface; it is estimated to lie at around −0.74 V (versus SCE) [29]. It is well-documented that lithium cations adsorb and intercalate into TiO_2 surface [30]. This lowers the energy of the conduction band edge and increases the driving force of the electron injection reaction. Therefore, in presence of lithium salt in the electrolyte, the free energy of the electron injection reaction becomes favourable with sensitizers **1** and **3**, whereas it can be thermodynamically limited with sensitizer **2** (Table 1). This is certainly a supplementary reason for the low photovoltaic efficiency observed with complex **2**.

3.4. Photoelectrochemical study

Complexes **1**–**3** were chemisorbed on nanocrystalline TiO_2 electrodes and were tested in wet DSSC (using the classical iodide/triiodide electrolyte) and in solid-state DSSC (using spin-coated layer of poly(octylthiophene) as hole conducting material). The meaningful characteristics of the solar cells are collected in Table 3.

We can notice that the new complex **3** displays the highest photovoltaic performances of the series both in wet and dry DSSCs. Therefore, the introduction of a non-conjugated spacer (ethanyl) between the terpyridine and the *tert*-thiophene unit has a beneficial impact on the photovoltaic performances of the sensitizer. The efficiency of complex **3** is even higher than that of the reference **1**. We can conclude that the *tert*-thiophene unit in complex **3** improves the efficiency of the cell because the short circuit photocurrent in the wet device and the Voc in both devices were increased with sensitizer **3** relative to sensitizer **1**. The Voc is a function of the recombination reactions between the injected electrons in the conduction band of TiO_2

Table 3
Photoelectrochemical characteristics of the complexes **1**–**3** measured in a sandwich type DSSC under simulated solar irradiation AM 1.5 (100 mW/cm^2)

Complex	Liquid electrolyte[a,b]				Solid-state device[c]			
	V_{oc} (V)	I_{sc} (mA cm^{-2})	ff (%)	η (%)	V_{oc} (V)	I_{sc} (μA cm^{-2})	ff (%)	η (%)
1	0.42	0.55	74	0.17	0.70	148	35	0.040
2	0.40	0.83	62	0.21	0.78	133	33	0.038
3	0.50	1.34	68	0.46	0.95	142	35	0.047

V_{oc}: open circuit; I_{sc}: short circuit photocurrent; ff: filling factor; η: overall photovoltaic efficiency.
[a] Composition of the liquid electrolyte: 0.05 M I_2, 0.5 M LiI, 0.1 M *tert*-butylpyridine in propylene carbonate.
[b] TiO_2 film of average thickness = 3 μm.
[c] TiO_2 film of average thickness = 1.5 μm.

with the oxidized sensitizers or with the redox mediator (I_3^- in wet cells or polythiophene in solid state cells). The complexes **1** and **3** display similar absorption spectra in the visible and similar excited-state redox potentials since the E (Ru^{III}/Ru^{II}) oxidation potentials and E_{00}(MLCT) of these complexes are almost identical (Table 1). It is therefore reasonable to postulate that these complexes, having the same anchoring group and the same molecular structure, should display similar electron injection quantum yield. As a result, the larger I_{sc} and the higher V_{oc} with **3** should probably stem from lower recombination reactions with the injected electron. It is a consequence of the probable charge shift reaction from the oxidized sensitizer (Ru^{III}) to the pendant *tert*-thiophene unit since there is a substantial driving force for this reaction (Table 1). The fast regeneration of the oxidized sensitizers and the removal of the positive charges away from the TiO_2 surface probably lead to a larger efficiency of the electron collection in the external circuit. Additionally, it is worthwhile to note that the V_{oc} is systematically higher in the solid-state devices compared to the wet cells (Table 3). Furthermore, in solid state cells the complex **3** leads to a larger V_{oc} than the reference sensitizer **1** lacking the *tert*-thiophene unit ($\Delta E = 250$ mV). These data highlight the usefulness of using a HTM displaying a higher oxidation potential than the couple iodide/triiodide and of functionalizing the sensitizer by a *tert*-thiophene unit. Although the overall photoconversion efficiency of these cells is still low with the present sensitizers, it is important to notice that the ruthenium sensitizers used in this study are far from being optimized in term of light harvesting efficiency and the utilization of other dyes exhibiting red-shifted absorption spectra combined with covalently linked HTM are promising systems for the development of solid-state dye-sensitized solar cells.

In conclusion, we have developed a straightforward synthetic route for the preparation of a ruthenium polypyridine sensitizer functionalized with a *tert*-thiophene unit attached though a non-conjugated ethanyl spacer. We demonstrated that the electronic independence of the ruthenium complex and the pendant oligothiophene unit is crucial to maintain the intrinsic sensitizing efficiency of the ruthenium complex. The impact of the ethanyl spacer is at least threefold. First, it restores the position of the LUMO orbitals on the anchoring terpyridine functionalized with phosphonic acid. Second, it interrupts the π-conjugation between the terpyridine and the *tert*-thiophene and limits the formation of the triplet $^3\pi$–π excited-state of the latter. Third, it leads to an increase of the energy of the MLCT and hence the electron injection driving force. These three factors certainly participate in the higher electron injection quantum yield. Additionally, the presence of an appended oligothiophene unit enhances the photovoltaic properties of the cell most probably owing to a decrease of the charge recombination processes. The most probable hole shift from the oxidized Ru(III) to the nearby *tert*-thiophene increases the separation distance between the positive charge (*tert*-thiophene$^+$) and the injected electron, which results in a lower dark current. Extended charge separated state lifetimes have been indeed observed in dyads containing a trisbipyridine ruthenium complexes functionalized by electron donors [31–34].

Ruthenium polypyridine complexes are still among the most efficient sensitizers for nanocrystalline TiO_2 DSSCs, therefore this finding could be valuable for the future design of molecular systems for solid-state DSSCs relying on π-conjugated conducting polymer.

Acknowledgements

Commissariat à l'Energie Atomique (CEA) and Région Pays de la Loire are gratefully acknowledged for the salary of C.H.-R.

References

[1] M.K. Nazeeruddin, P. Pechy, T. Renouard, S.M. Zakeeruddin, R. Humphry-Baker, P. Comte, P. Liska, L. Cevey, E. Costa, V. Shklover, L. Spiccia, G.B. Deacon, C.A. Bignozzi, M. Grätzel, J. Am. Chem. Soc. 123 (2001) 1613–1624.
[2] B. O'Regan, M. Grätzel, Nature 353 (1991) 737–739.
[3] M. Grätzel, J. Photochem. Photobiol. A: Chem. 164 (2004) 3–14.
[4] M.-S. Kang, J.H. Kim, Y.J. Kim, J. Won, N.-G. Park, Y.S. Kang, Chem. Commun. (2005) 889–891.
[5] A.F. Nogueira, J.R. Durrant, M.A. De Paoli, Adv. Mater. 13 (2001) 826–830.
[6] W. Kubo, S. Kambe, S. Nakade, T. Kitamura, K. Hanabusa, Y. Wada, S. Yanagida, J. Phys. Chem. B 107 (2003) 4374–4381.
[7] Q.-B. Meng, K. Takahashi, X.-T. Zhang, I. Sutanto, T.N. Rao, O. Sato, A. Fujishima, H. Watanabe, T. Nakamori, M. Uragami, Langmuir 19 (2003) 3572–3574.
[8] B. O'Regan, F. Lenzmann, R. Muis, J. Wienke, Chem. Mater. 14 (2002).
[9] U. Bach, D. Lupo, P. Comte, J.E. Moser, F. Weissörtel, J. Salbeck, H. Spreitzer, M. Grätzel, Nature 395 (1998) 583–585.
[10] N. Ikeda, T. Miyasaka, Chem. Commun. (2005) 1886–1888.
[11] K. Peter, H. Wietasch, B. Peng, M. Thelakkat, Appl. Phys. A 79 (2004) 65–71.
[12] K.R. Haridas, J. Ostrauskaite, M. Thelakkat, M. Heim, R. Bilke, D. Haarer, Synth. Met. 121 (2001) 1573–1574.
[13] A.F. Nogueira, C. Longo, M.A. De Paoli, Coord. Chem. Rev. 248 (2004) 1455–1468.
[14] L. Schmidt-Mende, M. Grätzel, Thin Solid Films 500 (2006) 296–301.
[15] Y. Saito, N. Fukuri, R. Senadeera, T. Kitamura, Y. Wada, S. Yanagida, Electrochem. Commun. 6 (2004) 71–74.
[16] C. Houarner, E. Blart, P. Buvat, F. Odobel, Photochem. Photobiol. Sci. 4 (2005) 200–204.
[17] T. Hayashi, M. Konishi, Y. Kobori, M. Kumada, T. Higuchi, K. Hirotsu, J. Am. Chem. Soc. 106 (1984) 158–163.
[18] T. Ukai, H. Kawazura, Y. Ishii, J.J. Bonnet, J.A. Ibers, J. Organomet. Chem. 65 (1974) 253–266.
[19] H.T. Uyeda, Y. Zhao, Wostyn, I. Asselberghs, K. Clays, A. Persoons, M.J. Therien, J. Am. Chem. Soc. 124 (2002) 13806–13813.
[20] S.M. Zakeeruddin, M.K. Nazeeruddin, P. Pechy, F.P. Rotzinger, R. Humphry-Baker, K. Kalyanasundaram, M. Grätzel, Inorg. Chem. 36 (1997) 5937–5946.
[21] S. Encinas, L. Flamigni, F. Barigelletti, E.C. Constable, C.E. Housecroft, E.R. Schofield, E. Figgemeier, D. Fenske, M. Neuburger, J.G. Vos, M. Zehnder, Chem. Eur. J. 8 (2002) 137–150.
[22] A. Barbieri, B. Ventura, F. Barigelletti, A. De Nicola, M. Quesada, R. Ziessel, Inorg. Chem. 43 (2004) 7359–7368.
[23] A. Barbieri, B. Ventura, L. Flamigni, F. Barigelletti, G. Fuhrmann, P. Bauerle, S. Goeb, R. Ziessel, Inorg. Chem. 44 (2005) 8033–8043.
[24] R. Ziessel, P. Bäuerle, M. Ammann, A. Barbieri, F. Barigelletti, Chem. Commun. (2005) 802–804.
[25] S.S. Zhu, R.P. Kingsborough, T.M. Swager, J. Mater. Chem. 9 (1999) 2123–2131.
[26] K.A. Walters, L. Trouillet, S. Guillerez, K.S. Schanze, Inorg. Chem. 39 (2000) 5496–5509.

[27] T.M. Pappenfus, K.R. Mann, Inorg. Chem. 40 (2001) 6301–6307.
[28] E.C. Glazer, D. Magde, Y. Tor, J. Am. Chem. Soc. 127 (2005) 4190–4192.
[29] G. Sauvé, M.E. Cass, G. Coia, S.J. Doig, I. Lauermann, K.E. Pomykal, N.S. Lewis, J. Phys. Chem. B 104 (2000) 6821–6836.
[30] C.A. Kelly, F. Farzad, D.W. Thompson, J.M. Stipkala, G.J. Meyer, Langmuir 15 (1999) 7047–7054.
[31] R. Argazzi, C.A. Bignozzi, T.A. Heimer, F.N. Castellano, G.J. Meyer, J. Phys. Chem. B 101 (1997) 2591–2597.
[32] P. Bonhôte, J.-E. Moser, R. Humphry-Baker, N. Vlachopoulos, S.M. Zakeeruddin, L. Walder, M. Grätzel, J. Am. Chem. Soc. 121 (1999) 1324–1336.
[33] N. Hirata, J.-J. Lagref, E.J. Palomares, J.R. Durrant, M.K. Nazeeruddin, M. Grätzel, D.D. Censo, Chem. Eur. J. 10 (2004) 595–602.
[34] S.A. Haque, S. Handa, K. Peter, E. Palomares, M. Telakkat, J.R. Durrant, Angew. Chem. Int. Ed. 44 (2005) 5740–5744.